

This document is the Accepted Manuscript version of a Published Work that appeared in final form in The Journal of Organic Chemistry, copyright © American Chemical Society after peer review and technical editing by the publisher. To access the final edited and published work see <https://doi.org/10.1021/acs.joc.1c00233>

An air-stable organic radical from a controllable photo-induced domino reaction of a hexa-aryl substituted anthracene

Xiaoyu Mao,[‡] Jianyu Zhang,[‡] Xiaohui Wang, Haoke Zhang, Peifa Wei, Herman H. Y. Sung, Ian D. Williams, Xing Feng,* Xin-Long Ni,* Carl Redshaw, Mark R. J. Elsegood, Jacky W. Y. Lam, Ben Zhong Tang*

Guangdong Provincial Key Laboratory of Functional Soft Condensed Matter, School of Material and Energy, Guangdong University of Technology, Guangzhou 510006, P. R. China

Department of Chemistry, The Hong Kong Branch of Chinese National Engineering Research Center for Tissue Restoration and Reconstruction, Institute for Advanced Study and Department of Chemical and Biological Engineering, The Hong Kong University of Science and Technology, Clear Water Bay, Kowloon, Hong Kong, China.

College of Chemistry and Chemical Engineering, Key Laboratory of the Assembly and Application of Organic Functional Molecules of Hunan Province, Hunan Normal University, Changsha 410081, P.R. China.

Department of Chemistry, University of Hull, Cottingham Road, Hull, Yorkshire HU6 7RX, UK.

Chemistry Department, Loughborough University, Loughborough LE11 3TU, UK.

KEYWORDS: *hexa-aryl anthracene, stable organic radical, iron (III)-catalyzed bromination, photo-induced domino reaction, electronic effect*

ABSTRACT: Stable organic radicals and radical ions have attracted great attention for their far-reaching application range from bioimaging to organic electronics. However, due to the highly reactive nature of organic radicals, the design and synthesis of air-stable organic radicals still remains a challenge. Herein, an air-stable organic radical from a controllable photo-induced domino reaction of a hexa-aryl substituted anthracene is described. The domino reaction involves a photo-induced [4+2] cycloaddition reaction, rearrangement, photolysis and an elimination reaction; ¹H/¹³C NMR spectroscopy, high resolution mass spectrometry (HRMS), single-crystal X-ray diffraction, as well as EPR spectroscopy were exploited for characterization. Furthermore, a photo-induced domino reaction mechanism is proposed according to the experimental and theoretical studies. In addition, the effects of employing push- and pull-electronic groups on the controllable photo-induced domino reaction were investigated. This article not only offers a new blue emitter and novel air-stable organic radical compound for potential application in organic semiconductor applications, but also provides a perspective for understanding the fundamentals of the reaction mechanism on going from anthracene to semiquinone in such anthracene systems.

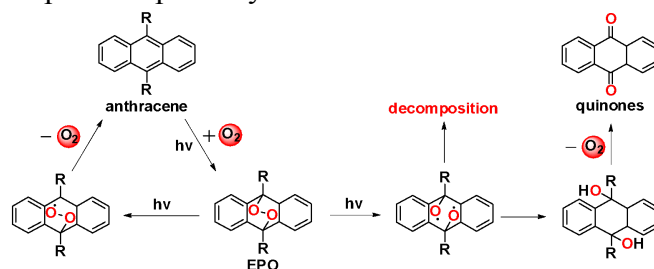
INTRODUCTION

Organic radicals are of fundamental interest given their relevance to organic reactions, molecular magnetism and spintronics, etc.¹⁻⁴ Moreover, the use of stable organic radicals and radical ions has led to advantages when utilized in the fields of organic light-emitting diodes,⁵⁻⁶ radical batteries,⁷ two-photon absorption materials^[8-9] and

biological probes.^{6,10} However, due to the highly reactive nature of organic radicals, the design and synthesis of rational molecular frameworks/conformations for stabilizing organic radicals still remains a challenge.¹¹ Generally, covalent approaches are commonly used for tuning the activity of organic radicals. For example, both the kinetic and thermodynamic stabilization of radicals can be efficiently achieved by steric protection and the delocalization of spin density on the organic molecules via covalent interactions. As a result, organic radicals exhibit great stability in the atmosphere (such as air and water) and can even be purified using silica columns and characterized by single crystal X-ray diffraction. More recently, Zeng and coworkers demonstrated that a domino reaction, which included 14 steps and formed up to 12 new covalent bonds could be used to synthesize a triarylmethyl radical.¹²

Anthracene is a representative member of the polycyclic aromatic hydrocarbons (PAHs), which are receiving great attention because of their potential application in both academic and industrial fields, e.g. organic semiconductors,^{13,14} and optical information storage.^{15,16} Unlike common PAH members, such as pyrene¹⁷ or perylene,¹⁸ the distinguishing characteristics of anthracene and its homologues are that they prefer to undergo a photo-induced [4+2] **cycloaddition** reaction with singlet oxygen (¹O₂) under irradiation, leading to endoperoxides (EPO).^{19,20} This further evolves into a competition between reconversion (to the parent acene) and decomposition.^[19-23] Thus, anthracenes can be widely utilized as high-efficiency trapping-releasing singlet oxygen agents for potential applications as high-performance photodynamic therapy agent (PDT)²³, fluorescent probes²⁴, molecular switches²⁵, as well as in lithography.²⁶

The mechanism of the photo-induced **cycloaddition** reaction of anthracene with oxygen has been exhaustively studied.^{20,22} Typically, photooxygenation of anthracenes occurs to give the corresponding 9,10-endoperoxides (EPOs), which further reform the parent anthracenes and undergo release of singlet oxygen (O₂ (a¹Δ_g)) through a cycloreversion process (Scheme 1).²⁷ On the other hand, photolysis of EPO can lead to decomposition to quinones by a multi-step cleavage process. The balance of this competition system can be broken by the specific substituents at the 9,10-positions of anthracene. Linker and co-worker previously observed that the alkynyl groups not only play a significant role in enhancing the stability of EPO, but also improve the conversion of EPO to the parent anthracenes in high yield.^{22,28} Very recently, Pan *et al.* found that 9,10-diarysubstituted anthracenes can transform *in-situ* into 5,5'-(anthracene-9,10-diyl)diisophthalic acid under hydrothermal conditions, and this was further confirmed by single-crystal X-ray diffraction.²⁹ Although the reaction mechanism is open to question, there is no doubt that the formation of various radical intermediates plays an important role in affecting the reaction pathway (such as photo-induced **cycloaddition** and photolysis reaction). However, how the substituents affect the photooxidations, photolysis and decomposition of anthracene, as well as details on the decomposition pathway and mechanism still remain unclear.



Scheme 1. The possible reaction pathways of the photo-induced **cycloaddition** reaction to anthracene endoperoxides (EPO), and the possible photo-induced cycloreversion and decomposition reaction of EPO.

The photo-induced chemical reaction always involves radical reactions, which leads to unidentified by-products via an un-controllable polymerization, addition, cleavage or decomposition reaction. In this article, we present a novel stable semiquinone radical, which was isolated from a controllable photo-induced domino reaction of a hexa-aryl substituted anthracene in three steps, involving in photo-induced **cycloaddition** reaction, a β -scission rearrangement and an elimination reaction. The semiquinone radical exhibited extreme stability, even under air (Temp. 25 °C, relative humidity: 50%-70%) for 1 year. The intermediate compounds were fully characterization by $^1\text{H}/^{13}\text{C}$ NMR spectra, high resolution mass spectrometry (HRMS), and single-crystal X-ray diffraction analysis, and this detailed information of the intermediates can help us to further understand the photo-induced domino reaction pathway; theoretical calculations were performed in order to clarify the photo-induced domino reaction mechanism. Thus, this article not only offers a straightforward strategy for the preparation of a stable radical for potential application in molecular electronics, but also provides evidence for understanding the reaction mechanism on going from anthracene to semiquinone via both experimental and theoretical techniques.

RESULTS AND DISCUSSION

Synthesis and characterization

According to the previously reported synthetic strategy,³⁰ we have developed a facile, widely applicable approach to the synthesis of novel D_{2h} symmetric hexaaryl substituted anthracenes **2** (see Figure 1). In the presence of iron powder, we found that bromination of anthracene or the 9-bromo anthracene under mild conditions such as stirring the reaction solution in CH_2Cl_2 at room temperature, can afford a yellow insoluble residue in high yield (71 %). In order to confirm the molecular conformation of these bromo-anthracene derivatives in detail, the bromo-anthracene precursor was directly utilized for the construction of novel anthracene derivatives *via* a Suzuki-Miyaura coupling reaction with the corresponding arylboronic acids. As expected, highly D_{2h} symmetric 2,3,6,7,9,10-hexa-aryl-substituted anthracenes **2** were afforded in considerable yield with good solubility in common organic solvents (such as CHCl_3 , toluene, THF and acetonitrile), and which were characterized by $^1\text{H}/^{13}\text{C}$ NMR spectroscopy, X-ray diffraction and high-resolution mass spectrometry (HRMS). Single crystals of **2a** and **2b** suitable for X-ray diffraction were grown *via* evaporation of a mixture of dichloromethane and hexane solution, and single crystal **2b'** was cultivated in a mixture of CHCl_3 and hexane solution. The six substituents were introduced at the 2-, 3-, 6-, 7-, 9- and 10-positions of the central anthracene core, which is agreement with our experimental results.

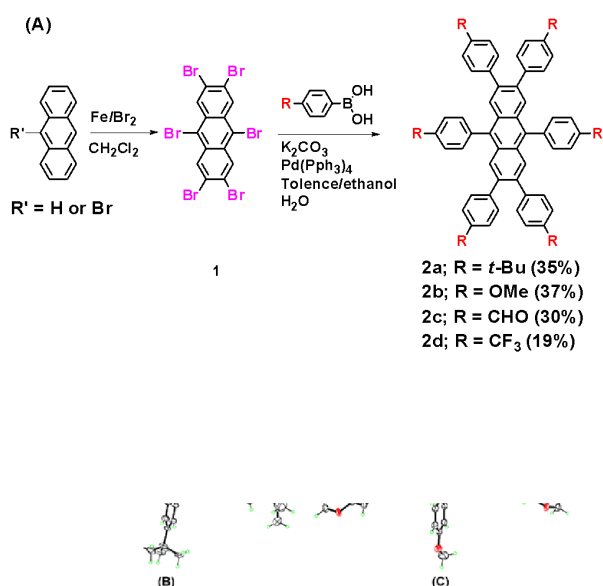


Figure 1 Synthetic route to 2,3,6,7,9,10-hexa-aryl-substituted anthracene derivatives (**2a-d**), and the single crystal structures of (A) **2a** and (B) **2b**, in ORTEP drawing with thermal ellipsoids at 30% probability.

Photophysical properties

The photophysical properties of **2a-d** were examined by UV-vis and fluorescence (PL) spectra in CH_2Cl_2 solution. As shown in Figure 2A, the four compounds exhibited similar absorption bands in the regions 280-350 nm and 370-450 nm, respectively. The short wavelength absorption region corresponded to the intramolecular charge transfer between the terminal groups at the 2-, 3-, 5-, 6-, 9- and 10-positions and the anthracene unit, while the long wavelength absorption band was assigned to π - π^* transitions of the anthracene core. The molar extinction coefficient of compounds **2-4** vary from 5.95×10^4 to $2.03 \times 10^5 \text{ cm}^{-1} \text{ M}^{-1}$. Clearly, the different electronic effects of the substituent groups at the 2-, 3-, 5-, 6-, 9- and 10-positions of the central anthracene core play a significant role in affecting the molar extinction coefficient (ϵ). With the substituents changing from a donating group **2a** (*t*-Bu), **2b** (OMe) to a withdrawing group **2c** (CHO), the absorption peaks are bathochromic shifted from 317 to 334 nm. In contrast, the compound **2d** (CF_3) with six of the strongest acceptor $-\text{CF}_3$ groups is blue shifted ~ 3 nm compared to that of **2a**, probably due to the effect of the dipole moment.^{31,32}

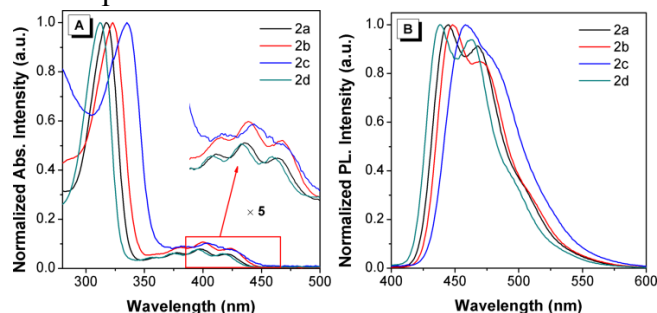


Figure 2. The UV-vis and PL spectra of hexa-aryl substituted anthracenes **2** in CH_2Cl_2 solution (10 μM) at 25 $^\circ\text{C}$

Upon excitation, all compounds emitted deep blue fluorescence both in solution and the solid state. As shown in Figure 2B, the photoluminescence (PL) spectra of

compound **2** illustrated a structureless emission band in the range 438-458 nm in CH₂Cl₂ solution with the order **2d** < **2a** < **2b** < **2c**, due to the electronic effect of the terminal group. For example, compound **2b** exhibited a maximum emission peak at 448 nm with a shoulder peak at 467 nm, attributed to the charge transfer character of the excited state.³³ In addition, the fluorescence quantum yields (Φ_f) of these compounds in CH₂Cl₂ solution were recorded and were found to vary from 0.46-0.59 (see Table S3). Thus, it can be concluded that iron-powder catalyzed the bromination of anthracene/9-bromo anthracene and this is a widely applicable strategy for preparing highly symmetric 2,3,6,7,9,10-hexabromoanthracenes with good regioselectivity, which have not been reported before and will be important intermediate compounds for the preparation of highly efficient anthracene-based organic semiconductor materials.

Photo-induced domino reaction of hexaaryl-substituted anthracenes

Normally, anthracene and its derivatives prefer to react with oxygen under UV-irradiation to afford EPOs, which further undergo a thermolysis or decomposition process with an uncontrollable reaction pathway.¹⁹⁻²² Here, to investigate the electronic effect on the kinetics of the photo-induced domino reaction these hexa-aryl substituted anthracenes, compounds **2** were irradiated ($\lambda_{\text{ex}}=365$ nm, 6 W) in CDCl₃ at 25 °C and tracked by ¹H NMR spectroscopy.

First step: Take **2b** as an example, as shown in Figure 3 and Figure S20, the ¹H NMR spectra clearly confirmed the molecular structure of **2b**, that is four doublets (24H) and one singlet (4H) were observed at 6.73, 7.03, 7.10, 7.45, 7.74 ppm which correspond to the protons of the anthracene and phenyl rings, respectively. After irradiation over 1 h, a new singlet proton peak appeared at a relatively low field position of 7.21 ppm, and four groups of doublets peaks were observed at 6.69, 6.90, 7.11 and 7.66 ppm, respectively, indicating that a new symmetrical compound was achieved. Subsequently, the intensity of the latter gradually increased as the proton signal of **2b** disappeared over 2 h under UV-irradiation. Finally, the compound **2b** ($m/z^+ = 814.339$) was quantitatively converted to the corresponding photoreactive species **3b** as determined by ¹H NMR spectroscopy. The molecular weight of **3b** was confirmed by HRMS with a molecular peak at $m/z^+ = 846.3172$ (Figure S46), indicating that the photoreactive species **3b** is an endoperoxide (EPO), formed by a photo-induced inter-molecular [4+2] cycloaddition reaction between compound **2b** with oxygen, which was also confirmed by single-crystal X-ray diffraction analysis (Figure 3B) (a single crystal of **3b** was obtained from a mixture of dichloromethane and hexane solution at room temperature). Interestingly, the photosensitive EPO **3b** can also be converted to **2b** as the temperature increases from 25 °C to 140 °C, which was tracked by a variable-temperature ¹H NMR spectroscopic study (Figure S31).

Second step: On prolonging the irradiation time from 2 h to 4 h, two new singlet peaks at 7.64 and 8.30 ppm and several new doublet peaks ($\delta = 6.75, 6.79, 7.03, 7.11, 7.37$ ppm) were observed. After irradiating for 5 h, the corresponding proton peaks of **3b** completely disappeared, and this compound was quantitatively converted to stable **4b** with a molecular ion peak of $m/z^+ = 741.24$ (Figure S47). A single crystal of **4b** was cultivated via solvent diffusion of hexane into a dichloromethane solution of the compound at room temperature. Furthermore, the effect of the irradiation powder, both in the presence/absence of oxygen, on the photo-induced domino reaction was investigated. ¹H NMR spectra indicated that EPO **3b** was different before and after increasing the irradiation time from 0 h to 10 h under a high UV power (100 W)

irradiation. Although we cannot identify the exact molecular structure of the new organic species **4b'**; according to the HRMS ($m/z^+ = 847.6789$), **4b'** can be assigned as an anthraquinone derivative and the proposed molecular structure is listed in Scheme S1. The product **4b'** exhibits extreme stability even under UV-irradiation 10 h ($\lambda_{\text{ex}} = 365$ nm, 100 W) (Figures S21-S24). This result inspired us to further explore this photo-induced domino reaction pathway.

Third step: The starting material **3b** (100 mg) was irradiated under a UV light ($\lambda_{\text{ex}} = 365$ nm, 6 W) for 4 h in chloroform and monitored by TLC. The resulting reaction mixture was further purified by silica gel column chromatography to afford a yellow powder **5b**, (15 mg, 18 % yield), although the ^1H NMR spectrum is similar with that of compound **4b** possessing two singlets and four doublets peaks at 8.30, 7.64, 7.37, 7.11, 7.03, 6.79 and 6.76 ppm in ratio of 2:2:2:4:4:6:4, respectively. Compared to the ^{13}C NMR spectrum of compounds **3b** and **4b**, the ^{13}C NMR spectrum at the C10 position of anthracene was shifted from 83.9 (**3b**) ppm to 183.3 ppm (**4b**), but the ^{13}C NMR spectrum of compounds **4b** and **5b** have slightly changed before and after UV irradiation (Figures S11, S17 and S20). The molecular ion of the **5b** ($m/z^+ = 723.2741$) (Figure S48) suggests the loss of a hydroxy group (OH) from compound **4b** ($m/z^+ = 741.24$). More importantly, from the FT-IR results, it is noted that the compound **5b** contains a clear C=O bond vibration peak at 1659 cm^{-1} , which is not observed in the FT-IR spectra of compounds **2b** and **3b** (Figure S36 and S37). This result provides more strong evidence for us to propose the exact molecular structure of semiquinone radical **5b** (Figure 3). We inferred that the OH group was captured in a separation process to afford **5b** which is thought to be due to the acidic nature of the silica gel column chromatography employed. Compound **5b** exhibited greater stability even under UV-light upon irradiating for 10 h in the absence/presence of O_2 (Figures S25-S28). However, the fluorescence spectra indicated that the emission intensity of **5b** was enhanced as the water fraction was increased. This result agrees with Pan's report (Figure S69).²⁹

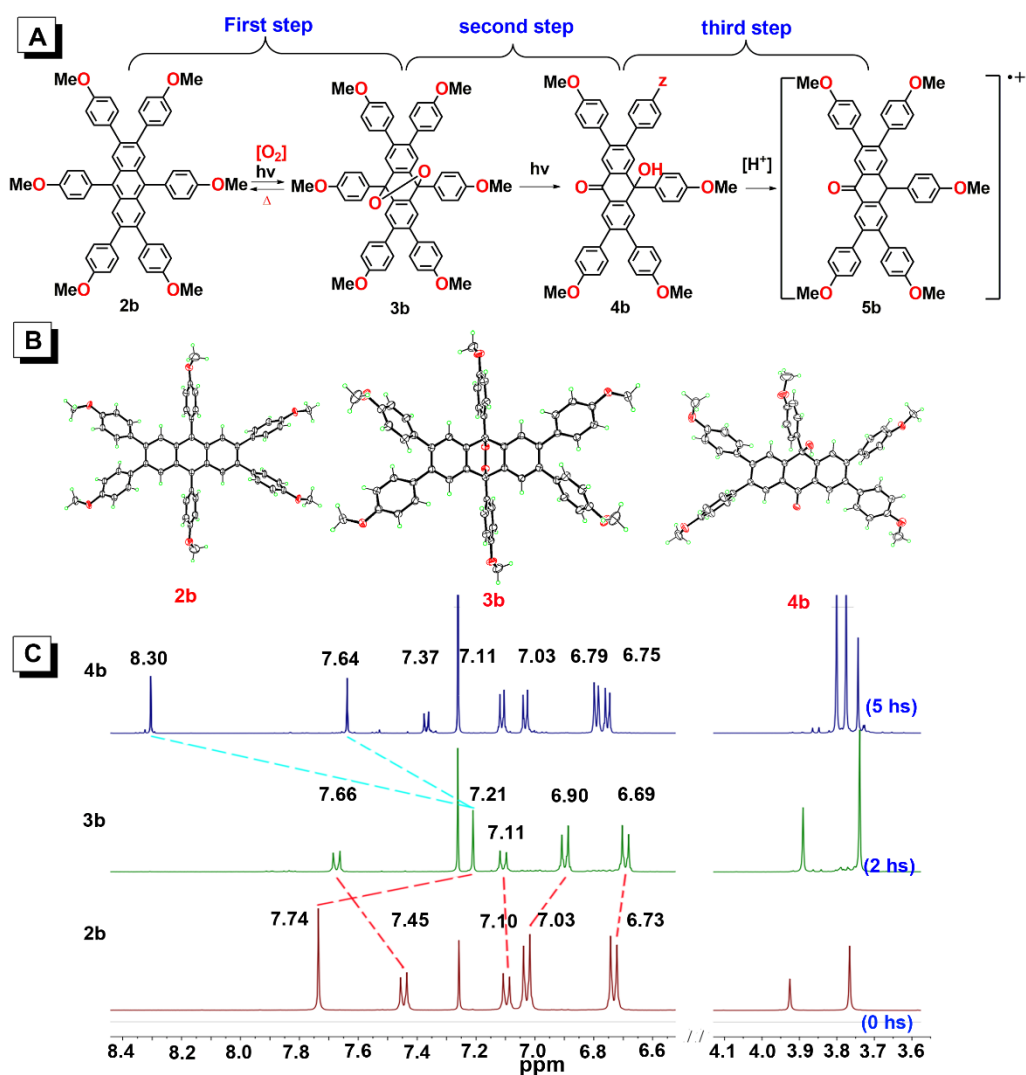


Figure 3. A) A controllable photo-induced domino reaction pathway from hexa-aryl substituted anthracene **2b** to **5b** under UV-irradiation ($\lambda_{\text{ex}} = 365 \text{ nm}$, 6W), B) X-ray single crystal structure of **2b** and its corresponding photo-induced products **3b** and **4b**, in ORTEP drawing with thermal ellipsoids at 30% probability, C) Irradiation time-dependent ^1H NMR spectra of photo-induced domino reaction from **2b** to **4b**.

EPR detection

In this hexaaryl anthracene systems, the entire photo-induced domino reaction processes were tracked by electron paramagnetic resonance (EPR) (Figure 4). After irradiation for 5 min., the solutions of **2b** and **3b** in toluene were measured using DMPO as the spin-trapping reagent. The spectra of **2b** show a weak signal, while a very clear EPR signal with a g value of 2.006 for **3b** in toluene was observed. The EPR spectra of **3b** was carefully calculated and fitted for assigning the type of radical. We found that the EPR signal contains three kinds of radical, including superoxide radical (O_2^-), self-photolysis of DMPO radical, and an alkyl radical upon comparing the database of radicals (Figure S38). On the other hand, the EPR spectra of both **2b** and **3b** in the solid state, before and after under UV irradiation for 10 min., did not reveal any signal. However, the spectra of **4b** showed a very weak signal in the solid state. It is interesting that the EPR studies of **5b** in the solid state at room temperature

showed a very strong paramagnetic signal with a g value of 2.007, which indicated that a radical cation does exist in **5b** (Figure 4A).³⁴ The EPR signal remains when compound **5b** was kept under air for 1 year, but the intensity of the EPR signal decreased somewhat, since trace water molecules are present in the external environment that can be captured by radical **5b** thereby forming **4b** (Figure 4B). More importantly, although the NMR spectra show slight changes, the EPR signal completely disappeared upon adding deuterium chloride (DCl, 35% in D₂O) to **5b** (Figure S39).

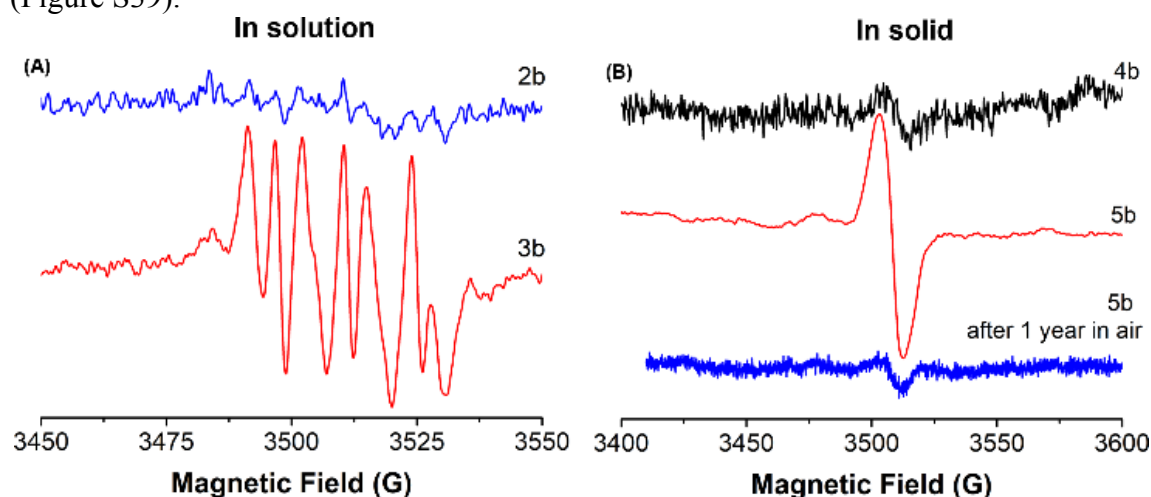


Figure 4. The EPR spectra of (A) compounds **2b** and **3b** ($g = 2.006$) in solution and (B) compounds **4b** ($g = 2.006$) and **5b** ($g = 2.007$) in the solid state at room temperature.

According to the single-crystal X-ray diffraction analysis, ¹H/¹³C NMR spectra, HRMS data as well as FT-IR spectra, the exact structure of products **2b-5b** were confirmed. Thus, a clearly controllable photo-induced domino reaction process with determined molecular structures can be outlined as in Figure 3A. Based on our knowledge, this is first such example of the hexaaryl anthracene systems, and offers a facile and efficient strategy for generating an air stable radical cation *via* a controllable photo-induced domino reaction under mild conditions.

The electronic effect on the photo-induced domino reaction

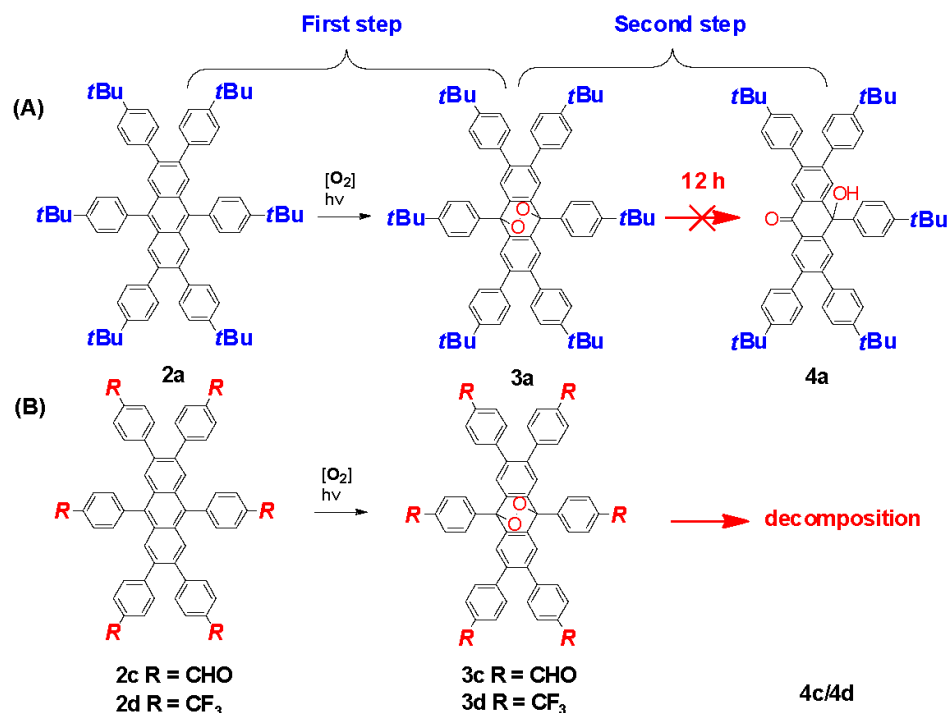


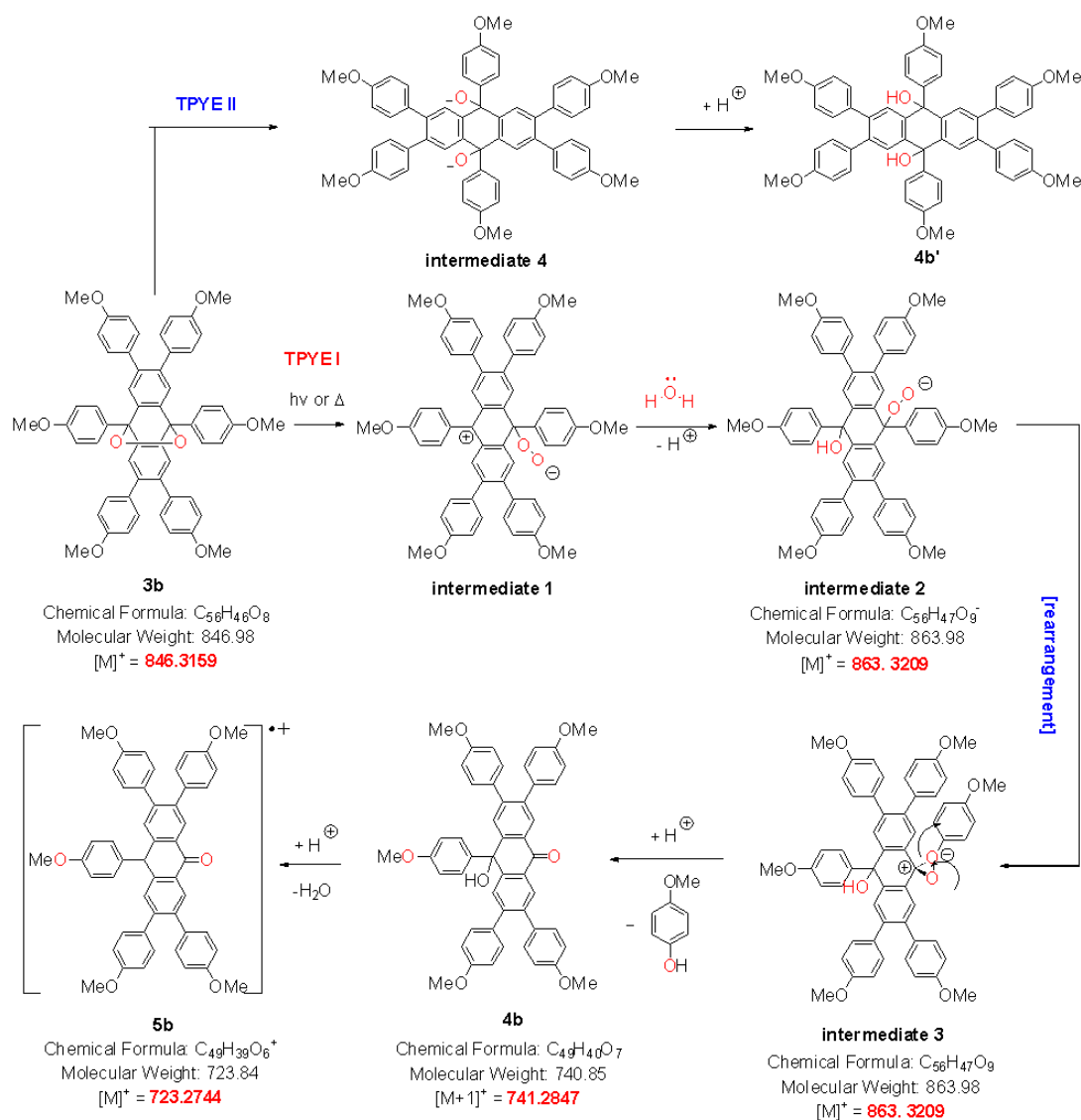
Figure 5 Two possible photo-induced reaction pathways (A) from hexa-aryl-substituted anthracene **2a** to EPO **3a** and (B) from hexa-aryl-substituted anthracenes **2c/2d** to decomposition under UV irradiation.

Previously, Linker and co-workers reported that EPO of anthracenes undergo a competitive reaction between reconversion and a decomposition process through either the homolysis of an O-O bond or cleavage of the C-O bond depending on the substituent group present at the 9,10-positions of the anthracene.²⁰ Therefore, possible photo-induced domino reactions of the hexaaryl-substituted anthracenes **2a**, **2c** and **2d** were also investigated under similar conditions to **2b** (UV light, $\lambda_{ex} = 356$ nm) and tracked by 1H NMR spectroscopy. As shown in Figure S19, in the presence of the weak electron-donating group, *tert*-butyl, five new proton peaks of **2a** ($\delta = 6.88, 7.13, 7.31, 7.58, 7.68$ ppm) were observed under UV irradiation for 20 min., which corresponded to the EPO **3a** ($m/z^+ = 1003.64$), whilst **2a** was totally converted to the EPO **3a** within 240 mins. Surprisingly, EPO **3a** is very stable and does not participate in the next photo-induced domino reaction to afford **4a** even under 12 h UV irradiation ($\lambda_{ex} = 365$ nm, 6W) (Figures S19, S43-44). This indicates that the presence of a *tert*-butyl group plays a significant role in stabilizing EPO **3a**.

Similarly, the hexaaryl-substituted anthracenes **2c** and **2d** can also be converted to their corresponding EPO **3c** ($m/z^+ = 834.88$) and **3d** ($m/z^+ = 1073.17$) within 90 min. and 180 min., respectively. However, the corresponding EPOs **3c** and **3d** are unstable and further cleavage of C-C may occur to afford decomposition (unidentified) compounds with $m/z^+ = 537.37$ for **4c** and $m/z^+ = 663.45$ for **4d**, respectively. As a result (Figure 5), it is concluded that the presence of a strong electron-withdrawing group can accelerate cleavage of the hexaaryl-substituted anthracenes and their frameworks. More importantly, it seems that the electron-donating units located at the 2,3,6,7,9,10-positions of anthracene can contribute to improve the reaction speed of the photo-induced inter-molecular [4+2] cycloaddition reaction (the first step) to form the photo-induced adduct compounds EPO in the order **2b** (60 min.) (>**2a** (240 min.)) > **2c** (180 min.) > **2d** (320 min.) (Figures S19-S30). Thus, we conclude that the

electronic effect plays a significant role to affect the pathway of the photo-induced domino reaction, and the strong electron-donating groups (-OMe) in this hexa-anthracene system would easily promote radical formation by a controllable photo-induced domino reaction, while the weak donating group (-*t*Bu) is beneficial to the stabilization of the EPO. In contrast, the electron-withdrawing groups (such as CHO or CF₃) would convert the anthracene derivative to an unknown product by an uncontrollable photo-induced decomposition process. Besides, it is believed that the strong electron-donating groups are beneficial to sufficiently stabilize the carbon-centered radical, which have borne out the prediction of Linker' *et al.*²⁰

Proposed photo-induced domino reaction mechanism



Scheme 2 The possible photo-induced domino reaction mechanism from hexaaryl-substituted anthracenes (**2a**) to stable radical-semiquinone radical **5b**; the m/z^+ in red color is the corresponding experimental results.

Based on the experimental data, we observed three possible reaction pathways for the thermolysis of EPO, depending on the electronic effect of the terminal groups. In order to obtain more insight into the mechanism for the hexaaryl-substituted anthracene systems *via* a photo-induced domino reaction pathway, combined experimental and DFT calculations were performed. The total energy of compound **2**

and EPO **3** were calculated using Gaussian 09 at the B3LYP theory level with 6-311G(d) basis set and ZPE corrections at 25 °C. The calculated thermodynamic energies of photo-induced inter-molecular [4+2] cycloaddition reaction from hexa-aryl anthracene **2** to EPO **3** were negative and are listed in Table S6. This indicates that the hexaaryl-substituted anthracenes **2** show high reactivity toward oxygen. Thus, combined with reported mechanism,¹⁹⁻²⁰ it is easier to understand why the mechanism of the photo-induced inter-molecular [4+2] cycloaddition reaction between hexaaryl-substituted anthracenes **2** and ¹O₂, affords the endoperoxides **3**.

On the other hand, to understand the electronic effect of the substituent group on the controllable photo-induced domino reaction mechanism, the highest occupied molecular orbitals (HOMO) and lowest unoccupied molecular orbitals (LUMO) of hexa-aryl anthracene **2** and EPO **3** were also calculated at the same theoretical level. On-going from the electron-donating groups (**2a** and **2b**) to the electron-withdrawn groups (**2c** and **2d**), the electron density distribution of these compounds progressively disperses from the central anthracene ring to the whole molecular framework. For example, the HOMO and LUMO of **2a** are mainly localized on the central anthracene ring, while the HOMO and LUMO of **2d** locate at both the anthracene core and over the substituent groups at the 2-, 3-, 6- and 8-positions (Table S7). The energy level of the HOMO was also raised following the order **2b** (OMe) > **2a** (*t*Bu) > **2c** (CHO) > **2d** (CF₃), which correlates with the photoactivity of the photo-induced inter-molecular [4+2] cycloaddition, and this result agrees with the report by Linker *et al.*²⁰

Experimental and theoretical methods have been used to thoroughly investigate the mechanism of the retro-reaction of EPO to the parent acene or to quinones (Scheme 1). Two possible mechanisms were proposed to clarify the photooxidation from acene to EPO, which is now generally accepted. However, the decomposition process of EPO to quinones still remains unclear. In our case, a new semiquinone **4b** was achieved by a controllable photo-induced domino reaction of the hexaaryl-substituted anthracene, which is beneficial in terms of understanding the mechanism of the photolysis to quinines in the anthracene system.

Moreover, variable-temperature ¹H NMR spectroscopy was performed in *d*-DMSO solution over the range 25 °C to 140 °C for tracking the thermolysis process (Figures S31 and S57). It was found that EPO **3b** quantitatively converted to **2b**. Due to the electron-donating 4-methoxyphenyl groups located at the 2-, 3-, 6-, 7-, 9- and 10-positions, the EPO **3b** exhibited a higher pyrolysis temperature compared to that of the 9,10-di-pyridine substituted anthracene derivatives.²⁸ Thus, according to the previously reports on the photolysis of anthracene^{22,25,29,35,36} and HRMS results, the possible photo-induced degradation intermediates here are summarized in Table S1.

Thus, three possible mechanisms for the metal-free catalyzed photo-induced domino reaction of hexaaryl-based anthracenes EPO are summarized in **Scheme 2**. In these hexaaryl-substituted anthracene systems, taking EPO **3b** as an example, after careful analysis of the experimental data (such as ¹H NMR, HRMS, EPR), it adopted two photolysis pathways depending on the power of the irradiation light. **Type I**: firstly, the photolysis of EPO prefers to proceed via an heterolytic cleavage of the C-O bond to form the **intermediate 1**; then a water molecule as a nucleophile was attacked, which resulting in **transition state 2**, and which further undergoes a β-scission reaction via a rearrangement process from **intermediate 3** to achieve **4b**³⁷, which is driven by solvent effects and the presence of the unstable three-membered ring system. Furthermore, a hydroxyl ion combines with a proton and then dissociates to achieve a stable radical cation **5b** with an sp² carbon center. **Type II**: The O-O bond

would break via a homolytic bond cleavage forming an extremely stable product **4b'** via an **intermediate 4** even under UV irradiation ($\lambda_{\text{ex}} = 365 \text{ nm}$, 100W), indicated that the barrier energy of homolytic O-O bond cleavage in the **Type II** pathway is higher than the heterolytic C-O bond cleavage process in the **Type I** pathway, meaning that the **Type II** pathway requires more energy expenditure. More importantly, the thermodynamic product **4b'** in **Type II** is more stable than **4b** of **Type I**, which is strongly supported by our experimental studies. **Type III**: due to the presence of an electron-withdrawing group, the intermediate carbon-centered radical is not stable in the homolytic O-O bond or heterolytic C-O bond cleavage process, which can undergo an uncontrollable photo-induced degradation reaction to afford unknown products. **Type III**: due to the presence of electron-withdrawing group, the intermediate with carbon-centered radical is not stable in the homolytic O-O bond or heterolytic C-O bond cleavage process, which would occur an uncontrollable photo-induced degradation reaction to achieve unknown products.

CONCLUSION

In this article, we firstly present a facile and controllable photo-induced domino reaction to obtain a stable organic radical from the 2,3,6,7,9,10-hexa-aryl substituted anthracene system, via an iron-catalyzed bromination and Suzuki-Miyaura cross-coupling reaction from anthracene. Due to the electronic effect of the substituents, the presence of donating groups such as the 4-*t*-butylphenyl group at the 2,3,6,7,9,10-positions of anthracene plays a significant role in stabilizing the endoperoxides (EPO), which then cannot be further involved in the photo-induced domino reaction to afford a radical. By contrast, in the presence of the electron donating group 4-methoxyphenyl, the photo-induced domino reaction in the 2,3,6,7,9,10-hexa-(4-methoxyphenyl) anthracene system exhibits a well-controlled process under UV irradiation to achieve a stable EPO, semiquinone, as well as a semiquinone radical, respectively. Molecular structures were confirmed by NMR spectra, HRMS and X-ray crystallography. However, with the strong electron withdrawing groups 4-formylphenyl and 4-trifluoromethyl, the anthracene derivatives prefer to undergo a photodegradation process affording unidentified compounds. Furthermore, a detailed photo-induced domino reaction mechanism was also proposed according to the theoretical study. This article not only offers a new blue emitter and novel air-stable organic radical compound for potential application in organic semiconductor applications, but also provides a perspective for understanding the fundamental knowledge on the photolysis pathway in such anthracene systems.

Experimental section

General information: ^1H and ^{13}C NMR spectra (400 MHz/ 600 MHz) were recorded on a Bruker AV 400/600 spectrometer, using chloroform-*d* solvent and SiMe_4 as internal reference. *J*-values are given in Hz. High-resolution mass spectra (HRMS) were taken on a LC/MS/MS, which consisted of a HPLC system (Ultimate 3000 RSLC, Thermo Scientific, USA) and a Q Exactive Orbitrap mass spectrometer, or taken on a GCT premier CAB048 mass spectrometer operating in a MALDI-TOF mode. Fluorescence spectra were recorded on a Hitachi F-4700 spectrofluorometer. UV-vis absorption spectra were obtained on a Milton Ray Spectrofluorometer. PL quantum yields were measured using absolute methods, using a Hamamatsu C11347-11 Quantaurus-QY Analyzer. EPR spectra were performed on a Bruker EMXplus-10/12 spectrometer. The quantum chemistry calculation was performed on the Gaussian 09W (B3LYP/6-31G** basis set) software package.^[38] Crystallographic data of the compounds were collected on a Bruker APEX 2 CCD diffractometer with

graphite monochromated Mo K α radiation ($\lambda = 0.71073 \text{ \AA}$) in the ω scan mode.^[39,40] The structure was solved by charge flipping or direct methods algorithms and refined by full-matrix least-squares methods, on F^2 .^[39] All esds (except the esd in the dihedral angle between two l.s. planes) are estimated using the full covariance matrix. The cell esds are taken into account individually in the estimation of esds in distances, angles and torsion angles. Correlations between esds in cell parameters are only used when they are defined by crystal symmetry. An approximate (isotropic) treatment of cell esds is used for estimating esds involving l.s. planes. The final cell constants were determined through global refinement of the xyz centroids of the reflections harvested from the entire data set. Structure solution and refinement were carried out using the SHELXTL-PLUS software package.^[39] Data (excluding structure factors) on the structures reported here have been deposited with the Cambridge Crystallographic Data Centre with deposition numbers. CCDC 1844505-1844506, 2052692-2052694 contain the supplementary crystallographic data for this paper. These data can be obtained free of charge from The Cambridge Crystallographic Data Centre via www.ccdc.cam.ac.uk/data_request/cif.

Materials: Unless otherwise stated, all other reagents used were purchased from commercial sources and were used without further purification. Tetrahydrofuran (THF) was distilled prior to use.

Synthesis of 2,3,6,7,9,10-hexa-bromoanthracene (1)

Run 1: A mixture of anthracene (530 mg, 3 mmol), iron powder (1.12 g, 20 mmol) and bromine (1.09 mL, 20 mmol) in dry CH₂Cl₂ (20 mL) was stirred under argon for 6 h at room temperature. The mixture was quenched with Na₂S₂O₃ (10%) and extracted with dichloromethane (50 mL \times 2). The combined organic extracts were washed by water and brine and evaporated, affording **1** (1.36 g, 71%) as a grey powder. The crude product is insoluble in common solvents and just slightly dissolved in hot CHCl₃. Due to the low solubility, the product was not further purified and was further used as the mixture for the Suzuki coupling reaction. HRMS (MALDI-TOF) m/z : [M CH]⁺ Calcd for C₁₄H₄Br₆, 651.61; found 662.7216.

Run2: A mixture of 9-bromo-anthracene (257 mg, 1 mmol), iron powder (0.40 g, 7 mmol) and bromine (0.3 mL, 5.5 mmol) in dry CH₂Cl₂ (20 mL) was stirred under argon for overnight at room temperature. The mixture was quenched with Na₂S₂O₃ (10%) and extracted with dichloromethane (50 mL \times 2). The combined organic extracts were washed by water and brine and evaporated. The crude product is insoluble in common solvent and just slightly dissolved in hot CHCl₃ (423 g, 65%) as a light grey powder, which was used without further purification.

General Procedure for 2,3,6,7,9,10-hexa-aryl substituted anthracene (2a-d)

Compounds **2a-d** were synthesized from 2,3,6,7,9,10-hexabromoanthracene (**1**) with the corresponding aryl boronic acid by a Suzuki coupling reaction in considerable yield.

Synthesis of 2,3,6,7,9,10-hexa-(4-tert-butylphenyl) anthracene (2a)

A mixture of 2,3,6,7,9,10-hexabromoanthracene (**1**) (320 mg, 0.5 mmol), 4-tert-butylphenyl boronic acid (600 mg, 3.4 mmol) in toluene (15 mL), ethanol (3 mL) and H₂O (3 mL) at room temperature was stirred under argon, and K₂CO₃ (500 mg, 3.6 mmol) and Pd(PPh₃)₄ (100 mg, 0.09 mmol) were added. After the mixture was stirred for 30 min. at room temperature under argon, the mixture was heated to 90 °C by oil bath, and stirred for 24 h. After cooling to room temperature, the mixture was quenched with water, extracted with CH₂Cl₂ (2 \times 30 mL), washed with water and brine. The organic extracts were dried with MgSO₄ and evaporated. The residue was purified by column chromatography eluting with CH₂Cl₂/hexane, 1:3 to give **2a** as a

light yellow powder (168 mg, 35 %). ^1H NMR (400 MHz, CDCl_3) δ 7.82 (s, 4H), 7.56 (d, $J = 8.1$ Hz, 4H), 7.46 (d, $J = 8.1$ Hz, 4H), 7.16 (d, $J = 8.1$ Hz, 8H), 7.00 (d, $J = 8.1$ Hz, 8H), 1.44 (s, 18H), 1.26 (s, 36H) ppm; $^{13}\text{C}\{^1\text{H}\}$ NMR (101 MHz, CDCl_3) δ 150.0, 149.2, 138.8, 138.4, 137.1, 135.7, 130.9, 129.8, 129.8, 128.0, 127.0, 125.7, 125.5, 124.4, 34.7, 34.4, 34.4, 31.5, 31.3; HRMS (FIMS+p ESI) m/z : $[\text{M}]^+$ Calcd for $\text{C}_{74}\text{H}_{82}$ 971.47; found 971.6452

A similar procedure with 4-methoxyphenylboronic acid, 4-formylphenylboronic acid, and 4-trifluoromethylphenylboronic acid was followed for the synthesis of **2b-2d**.

2,3,6,7,9,10-hexa-(4-methoxyphenyl) anthracene (2b) was obtained as a light yellow powder (152 mg, 37 %). ^1H NMR (400 MHz, CDCl_3) δ 7.73 (s, 4H), 7.44 (d, $J = 8.6$ Hz, 4H), 7.10 (d, $J = 8.6$ Hz, 4H), 7.03 (d, $J = 8.7$ Hz, 8H), 6.73 (d, $J = 8.7$ Hz, 8H), 3.92 (s, 3H), 3.76 ppm (s, 6H); $^{13}\text{C}\{^1\text{H}\}$ NMR (100 MHz, CDCl_3): $\delta = 158.9$, 158.3, 138.0, 136.4, 134.2, 132.3, 131.0, 130.9, 130.0, 128.1, 114.0, 113.3, 55.3, 55.2. ppm; HRMS (MALDI-TOF) m/z : $[\text{M}]^+$, Calcd for $\text{C}_{56}\text{H}_{46}\text{O}_6$ 814.33; found 814.3319.

2,3,6,7,9,10-hexa-(4-formylphenyl) anthracene (2c) was obtained as a yellow powder (122 mg, 30 %). ^1H NMR (400 MHz, CDCl_3): $\delta_{\text{H}} = 10.19$ (s, 2H), 9.95 (s, 4H), 8.18 (d, $J = 8.1$ Hz, 4H), 7.78 (d, $J = 8.0$ Hz, 4H), 7.71 (d, $J = 8.3$ Hz, 8H), 7.23 ppm (d, $J = 8.2$ Hz, 8H); $^{13}\text{C}\{^1\text{H}\}$ NMR (100 MHz, CDCl_3): $\delta = 191.6$, 146.5, 144.3, 138.1, 137.1, 136.2, 135.0, 131.9, 130.3, 130.3, 129.6, 129.5, 128.7 ppm; HRMS (FIMS-pAPCI) m/z : $[\text{M}^+ + 1]$, Calcd for $\text{C}_{56}\text{H}_{34}\text{O}_6$ 802.2355; found 803.2430.

2,3,6,7,9,10-hexa-(4-trifluoromethyl) anthracene (2d) was obtained as a yellow powder (98 mg, 19 %). ^1H NMR (400 MHz, CDCl_3) δ 7.91 (d, $J = 7.6$ Hz, 4H), 7.70 (d, $J = 7.9$ Hz, 4H), 7.67 (s, 4H), 7.48 (d, $J = 8.0$ Hz, 8H), 7.18 (d, $J = 8.0$ Hz, 8H). $^{13}\text{C}\{^1\text{H}\}$ NMR (101 MHz, CDCl_3) δ 144.0, 141.7, 137.9, 136.7, 131.6, 131.5, 130.0, 129.6, 129.3, 128.6, 127.6, 126.0, 125.2, 125.2; HRMS (FIMS-pAPCI) m/z : $[\text{M}]^+$ Calcd for $\text{C}_{56}\text{H}_{28}\text{O}_{18}$ 1042.79; found 1042.1929

Synthesis of Endoperoxide **3a**

Compound **2a** (10 mg, 0.01 mmol) in CDCl_3 (0.5 mL) in a NMR tube was kept under UV light ($\lambda_{\text{ex}} = 365\text{nm}$) irradiation and this reaction process was tracked by ^1H NMR spectroscopy. After 60 mins, the compound **2a** was converted to **3a** in quantitative yield (11 mg, 100%) as a deep yellow powder. ^1H NMR (400 MHz, CDCl_3) δ 7.68 (d, $J = 8.4$ Hz, 4H), 7.59 (s, 4H), 7.31 (s, 4H), 7.13 (d, $J = 8.2$ Hz, 8H), 6.88 (d, $J = 8.2$ Hz, 8H), 1.39 (d, $J = 9.9$ Hz, 18H), 1.24 (s, 36H); $^{13}\text{C}\{^1\text{H}\}$ NMR (101 MHz, CDCl_3) δ 150.9, 149.4, 140.1, 139.4, 138.2, 129.7, 129.6, 129.4, 127.0, 127.0, 125.5, 124.8, 124.5, 84.1, 34.8, 34.4, 31.4, 31.3(s); HRMS (FTMS + p APCI) m/z : $[\text{M}]^+$ Calcd for $\text{C}_{74}\text{H}_{82}\text{O}_2$ 1003.47; found 1003.6418.

Synthesis of Endoperoxide **3b**

Method 1: Compound **2b** (10 mg, 0.01 mmol) in CDCl_3 (0.5 mL) in a NMR tube was kept under UV light ($\lambda_{\text{ex}} = 365\text{nm}$) irradiation and this reaction process was tracked by ^1H NMR spectroscopy. After 2 h, the compound **2b** was converted to **3b** in quantitative yield (10 mg, 100%) as a yellow powder. ^1H NMR (400 MHz, CDCl_3): $\delta_{\text{H}} = 7.67$ (d, $J = 8.9$ Hz, 4H), 7.21 (s, 4H), 7.11 (d, $J = 8.9$ Hz, 4H), 6.90 (d, $J = 8.7$ Hz, 8H), 6.69 (d, $J = 8.8$ Hz, 8H), 3.89 (s, 6H), 3.74 ppm (s, 12H); $^{13}\text{C}\{^1\text{H}\}$ NMR (100 MHz, CDCl_3): $\delta = 159.2$, 158.3, 139.6, 139.3, 133.6, 130.9, 128.5, 125.7, 124.8, 113.9, 113.4, 83.9, 55.3, 55.2 ppm; HRMS (MALDI-TOF): m/z $[\text{M}]^+$ Calcd for $\text{C}_{56}\text{H}_{46}\text{O}_8$ 846.32; found 846.3172.

Method 2: The compound **2b** (100 mg, 0.12 mmol) was dissolved in CHCl_3 (30 mL) in a beaker and stirred, the solution was kept under visible light irradiation (simulated sunlight irradiation) and this reaction process was tracked by TLC. After 2 h, the

solution was evaporated and purified by column chromatography eluting with CH₂Cl₂ to give **3b** as a yellow powder (82 mg, 79 %). ¹H NMR (400 MHz, CDCl₃): δ_H = 7.67 (d, *J* = 8.9 Hz, 4H), 7.21 (s, 4H), 7.11 (d, *J* = 8.9 Hz, 4H), 6.90 (d, *J* = 8.7 Hz, 8H), 6.69 (d, *J* = 8.8 Hz, 8H), 3.89 (s, 6H), 3.74 ppm (s, 12H).

Synthesis of Endoperoxide **3c**

Compound **2c** (10 mg, 0.01 mmol) in CDCl₃ (0.5 mL) in a NMR tube was kept under UV light (λ_{ex} = 365nm) irradiation and this reaction process was tracked by ¹H NMR spectroscopy. After 1 h, the compound **2c** was converted to **3c** in quantitative yield (11 mg) as a light yellow powder. ¹H NMR (400 MHz, CDCl₃): δ 10.15 (s, 2H), 9.93 (s, 4H), 8.19 (d, *J* = 8.4 Hz, 4H), 7.98 (d, *J* = 8.3 Hz, 4H), 7.68 (d, *J* = 8.3 Hz, 8H), 7.23 (s, 4H), 7.12 ppm (d, *J* = 8.2 Hz, 8H); ¹³C{¹H} NMR (100 MHz, CDCl₃): δ = 191.5, 145.9, 139.7, 139.3, 138.1, 136.6, 135.2, 135.0, 131.9, 130.3, 130.1, 129.7, 129.6, 128.7, 128.0, 125.6, 83.9 ppm; HRMS (MALDI-TOF) *m/z*: [M+1]⁺ Calcd for C₅₆H₃₄O₈ 834.23; found 835.2200

Synthesis of Endoperoxide **3d**

Compound **2d** (10 mg, 0.01 mmol) in CDCl₃ (0.5 mL) in a NMR tube was kept under UV light (λ_{ex} = 365nm) irradiation and this reaction process was tracked by ¹H NMR spectroscopy. After 1 h, the compound **2d** was converted to **3d** in quantitative yield (11 mg) as a dark yellow powder. ¹H NMR (400 MHz, CDCl₃) δ 7.92 (dd, *J* = 15.6, 8.0 Hz, 2H), 7.45 (d, *J* = 8.1 Hz, 2H), 7.18 (s, 1H), 7.07 (d, *J* = 8.0 Hz, 2H). ¹³C{¹H} NMR (101 MHz, CDCl₃) δ 143.4, 139.5, 139.2, 135.7, 130.0, 129.8, 129.5, 127.7, 127.6, 126.0, 125.7, 125.4, 122.5; HRMS (FTMS-p APCI) *m/z*: [M]⁺ Calcd for C₅₆H₃₀F₁₈O₂ 1076.83; found 1077.1604.

Synthesis of semiquinone **4b**

The aboved compound **3b** (Method 1, 10 mg, 0.01 mmol) in an NMR tube in CDCl₃ solution was irradiated under a UV light and monitored by ¹H NMR spectroscopy. After 2.5 h, the compound **3b** was converted to **4b** in quantitative yield (9 mg) as a yellow powder. ¹H NMR (600 MHz, CDCl₃): 8.30 (s, 2H), 7.64 (s, 2H), 7.37 (d, *J* = 8.9 Hz, 2H), 7.11 (d, *J* = 8.7 Hz, 4H), 7.03 (d, *J* = 8.7 Hz, 4H), 6.79 (d, *J* = 8.6 Hz, 6H), 6.76 (t, *J* = 5.8 Hz, 4H), 3.80 (s, 3H), 3.77 (s, 3H), 3.74 (s, 3H). ¹³C NMR (151 MHz, CDCl₃) δ 183.3, 180.6, 158.9, 158.6, 158.4, 146.6, 145.8, 140.2, 138.3, 132.9, 132.7, 130.9, 130.3, 129.0, 128.8, 126.9, 126.8, 116.0, 114.8, 113.8, 113.6, 113.5, 113.5, 113.3, 72.9, 55.2 ppm. HRMS (MALDI-TOF)*m/z* : [M]⁺ Calcd for C₄₉H₄₀O₇ 740.85. found 740.2774.

Synthesis of radical **5b**

The starting material **3b** (100 mg) was irradiated under a UV light (365nm) 4 h in chloroform and monitored by TLC. The resulting reaction mixture was further purified by silica gel column chromatography affording a yellow powder in 15 mg (18% yield). ¹H NMR (600 MHz, CDCl₃) δ 8.30 (s, 2H), 7.64 (s, 2H), 7.37 (d, *J* = 8.9 Hz, 2H), 7.11 (d, *J* = 8.7 Hz, 4H), 7.03 (d, *J* = 8.7 Hz, 4H), 6.79 (d, *J* = 8.7 Hz, 6H), 6.75 (d, *J* = 8.7 Hz, 2H), 3.80 (s, 6H), 3.78 (s, 6H), 3.74 (s, 3H) ppm. ¹³C{¹H} NMR (151 MHz, CDCl₃) δ 183.3, 158.9, 158.7, 158.3, 146.6, 145.7, 140.1, 138.3, 132.9, 132.7, 130.9, 130.2, 129.0, 128.8, 126.8, 113.8, 113.6, 113.5, 72.9, 55.2, 55.2, 53.4 ppm. HRMS (MALDI-TOF) *m/z* : [M]⁺ Calcd for C₄₉H₃₉O₆⁺ 723.84; found 723.2741.

ASSOCIATED CONTENT

Supporting Information

The Supporting Information is available free of charge on the ACS Publications website.

Additional experimental methods for the hexa-anthracene derivatives. Details of the experimental characterization, including $^1\text{H}/^{13}\text{C}$ NMR spectra, HRMS, Results of UV-vis and fluorescence spectra, DFT calculations (PDF)

Single crystal X-ray diffraction of **2a**, **2b**, **3b** and **4b** (CIF)

AUTHOR INFORMATION

Corresponding Author

Xing Feng- Guangdong Provincial Key Laboratory of Functional Soft Condensed Matter, School of Material and Energy, Guangdong University of Technology, Guangzhou 510006, P. R. China. E-mail: hyxhn@sina.com

Ben Zhong Tang - Department of Chemistry, The Hong Kong Branch of Chinese National Engineering Research Center for Tissue Restoration and Reconstruction, Institute for Advanced Study and Department of Chemical and Biological Engineering, The Hong Kong University of Science and Technology, Clear Water Bay, Kowloon, Hong Kong, China. E-mail: tangbenz@ust.hk

Xin-Long Ni- College of Chemistry and Chemical Engineering, Key Laboratory of the Assembly and Application of Organic Functional Molecules of Hunan Province, Hunan Normal University, Changsha 410081, P.R. China. E-mail: longni333@163.com

Author

Xiaoyu Mao- Guangdong Provincial Key Laboratory of Functional Soft Condensed Matter, School of Material and Energy, Guangdong University of Technology, Guangzhou 510006, P. R. China

Jianyu Zhang- Department of Chemistry, The Hong Kong Branch of Chinese National Engineering Research Center for Tissue Restoration and Reconstruction, Institute for Advanced Study and Department of Chemical and Biological Engineering, The Hong Kong University of Science and Technology, Clear Water Bay, Kowloon, Hong Kong, China.

Xiaohui Wang- Guangdong Provincial Key Laboratory of Functional Soft Condensed Matter, School of Material and Energy, Guangdong University of Technology, Guangzhou 510006, P. R. China

Haoke Zhang- Department of Chemistry, The Hong Kong Branch of Chinese National Engineering Research Center for Tissue Restoration and Reconstruction, Institute for Advanced Study and Department of Chemical and Biological Engineering, The Hong Kong University of Science and Technology, Clear Water Bay, Kowloon, Hong Kong, China.

Peifa Wei- Department of Chemistry, The Hong Kong Branch of Chinese National Engineering Research Center for Tissue Restoration and Reconstruction, Institute for Advanced Study and Department of Chemical and Biological Engineering, The Hong Kong University of Science and Technology, Clear Water Bay, Kowloon, Hong Kong, China.

Herman H. Y. Sung- Department of Chemistry, The Hong Kong Branch of Chinese National Engineering Research Center for Tissue Restoration and Reconstruction, Institute for Advanced Study and Department of Chemical and Biological

Engineering, The Hong Kong University of Science and Technology, Clear Water Bay, Kowloon, Hong Kong, China.

Ian D. Williams- Department of Chemistry, The Hong Kong Branch of Chinese National Engineering Research Center for Tissue Restoration and Reconstruction, Institute for Advanced Study and Department of Chemical and Biological Engineering, The Hong Kong University of Science and Technology, Clear Water Bay, Kowloon, Hong Kong, China.

Carl Redshaw- Department of Chemistry, University of Hull, Cottingham Road, Hull, Yorkshire HU6 7RX, UK.

Mark R. J. Elsegood- Chemistry Department, Loughborough University, Loughborough LE11 3TU, UK.

Jacky W. Y. Lam- Department of Chemistry, The Hong Kong Branch of Chinese National Engineering Research Center for Tissue Restoration and Reconstruction, Institute for Advanced Study and Department of Chemical and Biological Engineering, The Hong Kong University of Science and Technology, Clear Water Bay, Kowloon, Hong Kong, China.

Author Contributions

‡These authors contributed equally.

Notes

The authors declare no competing financial interest.

ACKNOWLEDGMENT

This work was supported by the National Natural Science Foundation of China (21975054 and 21602014), Natural Science Foundation of Guangdong Province of China (2019A1515010925), “One Hundred Talents Program” of the Guangdong University of Technology (GDUT) (1108-220413205), the Research Grants Council of Hong Kong (C6009-17G), and the Innovation of Technology Commission (ITC-CNERC14SC01). CR thanks the EPSRC for an Overseas Travel Grant (EP/R023816/1). We thank Dr. Menglong Zhang (South China Normal University), Mr. Hang Li (Test Center of Guangdong University of Technology) for helpful discussions.

REFERENCES

- [1] Koide, T.; Kashiwazaki, G.; Suzuki, M.; Furukawa, K.; Yoon, M.-C.; Cho, S.; Kim, D.; Osuka, A. A Stable Radical Species from Facile Oxygenation of meso-Free 5,10,20,25-Tetrakis(pentafluorophenyl)-Substituted [26]Hexaphyrin(1.1.1.1.1.1). *Angew. Chem. Int. Ed.* **2008**, *120*, 9807-9811.
- [2] Ito, A.; Shimizu, A.; Kishida, N.; Kawanaka, Y.; Kosumi, D.; Hashimoto, H.; Teki, Y.; Excited-State Dynamics of Pentacene Derivatives with Stable Radical Substituents. *Angew. Chem. Int. Ed.* **2014**, *53*, 6715-6719.
- [3] Wang, Y.; Frasconi, M.; Stoddart, J. F.; Introducing Stable Radicals into Molecular Machines. *ACS Cent. Sci.* **2017**, *3*, 927-935.
- [4] Mas-Torrent, M.; Crivillers, N.; Rovira, C.; Veciana, J.; Attaching Persistent Organic Free Radicals to Surfaces: How and Why. *Chem. Rev.* **2012**, *112*, 2506-2527.
- [5] Bin, Z.; Liu, Z.; Duan, L.; Organic Radicals Outperform LiF as Efficient Electron-Injection Materials for Organic Light-Emitting Diodes. *J. Phys. Chem. Lett.* **2017**, *8*, 4769-4773.

- [6] Ai, X.; Evans, E. W.; Dong, S.; Gillett, A. J.; Guo, H.; Chen, Y.; Hele, T. J. H.; Friend, R. H.; Li, F.; Efficient radical-based light-emitting diodes with doublet emission. *Nature*, **2018**, *563*, 536-540.
- [7] Morita, Y.; Nishida, S.; Murata, T.; Moriguchi, M.; Ueda, A.; Satoh, M.; Arifuku, K.; Sato, K.; Takui, T.; Organic tailored batteries materials using stable open-shell molecules with degenerate frontier orbitals. *Nat. Mater.* **2011**, *10*, 947-951.
- [8] Kamada, K.; Ohta, K.; Kubo, T.; Shimizu, A.; Morita, Y.; Nakasuji, K.; Kishi, R.; Ohta, S.; Furukawa, S.; Takahashi, H.; Nakano, M.; Strong Two-Photon Absorption of Singlet Diradical Hydrocarbons. *Angew. Chem., Int. Ed.* **2007**, *46*, 3544-3546.
- [9] Kamada, K.; Fuku-en, S.-i.; Minamide, S.; Ohta, K.; Kishi, R.; Nakano, M.; Matsuzaki, H.; Okamoto, H.; Higashikawa, H.; Inoue, K.; Kojima, S.; Yamamoto, Y. Impact of Diradical Character on Two-Photon Absorption: Bis(acridine) Dimers Synthesized from an Allenic Precursor. *J. Am. Chem. Soc.* **2013**, *135*, 232-241.
- [10] Eroglu, E.; Gottschalk, B.; Charoensin, S.; Blass, S.; Bischof, H.; Rost, R.; Madreiter-Sokolowski, C. T.; Pelzmann, B.; Bernhart, E.; Sattler, W.; Hallström, S.; Malinski, T.; Waldeck-Weiermair, M.; Graier, W. F.; Malli, R. Development of novel FP-based probes for live-cell imaging of nitric oxide dynamics. *Nat. Commun.* **2016**, *7*, 10623.
- [11] Nobusue, S.; Miyoshi, H.; Shimizu, A.; Hisaki, I.; Fukuda, K.; Nakano, M.; Tobe, Y. Tetracyclopenta[def,jkl,pqr,vwx]tetraphenylene: A Potential Tetraradicaloid Hydrocarbon. *Angew. Chem., Int. Ed.* **2015**, *54*, 2090-2094.
- [12] Liu, B.; Yu, F.; Tu, M.; Zhu, Z.-H.; Zhang, Y.; Ouyang, Z.-W.; Wang, Z.; Zeng, M.-H.; Tracking the Process of a Solvothermal Domino Reaction Leading to a Stable Triheteroarylmethyl Radical: A Combined Crystallographic and Mass-Spectrometric Study. *Angew. Chem., Int. Ed.* **2019**, *58*, 3748-3753.
- [13] Yoshizawa, M.; Klosterman, J. K.; Molecular architectures of multi-anthracene assemblies. *Chem. Soc. Rev.* **2014**, *43*, 1885-189.
- [14] Huang, J.; Su, J.-H.; Tian, H.; The development of anthracene derivatives for organic light-emitting diodes. *J. Mater. Chem.* **2012**, *22*, 10977-10989.
- [15] Wu, J.; Pisula, W.; Müllen, K. Graphenes as Potential Material for Electronics. *Chem. Rev.* **2007**, *107*, 718-747.
- [16] Dini, D.; Calvete, M. J. F.; Hanack, M. Nonlinear Optical Materials for the Smart Filtering of Optical Radiation. *Chem. Rev.* **2016**, *116*, 13043-13233.
- [17] a) Feng, X.; Hu, J.-Y.; Redshaw, C.; Yamato, T.; Functionalization of pyrene to Advanced Luminescence Materials - A review of Methodology. *Chem. Eur. J.* **2016**, *22*, 11898-11916; b) Islam, M. M.; Hu, Z.; Wang, Q.; Redshaw, C.; Feng, X. Pyrene-based aggregation-induced emission luminogens and their applications. *Mater. Chem. Front.* **2019**, *3*, 762-781.
- [18] Markiewicz, J. T.; Wudl, F. Perylene, Oligorylenes, and Aza-Analogs. *ACS Appl. Mater. Interfaces* **2015**, *7*, 28063-28085.
- [19] Donkers, R. L.; Workentin, M. S.; Elucidation of the Electron Transfer Reduction Mechanism of Anthracene Endoperoxides. *J. Am. Chem. Soc.* **2004**, *126*, 1688-1698.
- [20] a) Fudickar, W.; Linker, T. Why Triple Bonds Protect Acenes from Oxidation and Decomposition. *J. Am. Chem. Soc.* **2012**, *134*, 15071-15082; b) Zhao, J.-L.; Wu, C.; Tomiyasu, H.; Zeng, X.; Elsegood, M. R. J.; Redshaw, C.; Yamato, T. A Rare and Exclusive Endoperoxide Photoproduct Derived from a Thiocalix[4]arene Crown-Shaped Derivative Bearing a 9,10-Substituted Anthracene Moiety, *Chemistry Asian J.*, **2016**, *11*, 1606-1612

- [21] Martinez, G. R.; Ravanat, J.-L.; Cadet, J.; Miyamoto, S.; Medeiros, M. H. G.; Mascio, P. D.; Catalytic Nanomotors: Autonomous Movement of Striped Nanorods. *J. Am. Chem. Soc.* **2004**, *126*, 3056-3057.
- [22] Arian, D.; Kovbasyuk, L.; Mokhir, A. 1,9-Dialkoxyanthracene as a 1O₂-Sensitive Linker. *J. Am. Chem. Soc.* **2011**, *133*, 3972–3980.
- [23] Kolemen, S.; Ozdemir, T.; Gyoung, D. L.; Kim, M.; Karatas, T.; Yoon, J.; Akkaya, E. U.; Remote-Controlled Release of Singlet Oxygen by the Plasmonic Heating of Endoperoxide-Modified Gold Nanorods: Towards a Paradigm Change in Photodynamic Therapy. *Angew. Chem. Int. Ed.* **2016**, *55*, 3606–3610.
- [24] Pedersen, S. K.; Holmehave, J.; Blaikie, F. H.; Gollmer, A.; Breitenbach, T.; Jensen, H. H.; Ogilby, P. R.; Aarhus Sensor Green: A Fluorescent Probe for Singlet Oxygen. *J. Org. Chem.* **2014**, *79*, 3079–3087.
- [25] Zehm, D.; Fudickar, W.; Linker, T.; Molecular Switches Flipped by Oxygen. *Angew. Chem. Int. Ed.* **2007**, *46*, 7689-7692.
- [26] Fudickar, W.; Linker, T. Novel Anthracene Materials for Applications in Lithography and Reversible Photoswitching by Light and Air. *Langmuir* **2010**, *26*, 4421-4428.
- [27] Aubry, J.-M.; Pierlo, C.; Rigaudy, J.; Schmidt, R.; Reversible Binding of Oxygen to Aromatic Compounds. *Acc. Chem. Res.* **2003**, *36*, 668–675.
- [28] Liu, K.; Lalancette, R. A.; Jäkle, F. B–N Lewis Pair Functionalization of Anthracene: Structural Dynamics, Optoelectronic Properties, and O₂ Sensitization. *J. Am. Chem. Soc.* **2017**, *139*, 50, 18170–18173.
- [29] Gu, D.; Yang, W.; Ning, G.; Wang, F.; Wu, S.; Shi, X.; Wang, Y.; Pan, Q. In Situ Ligand Formation-Driven Synthesis of a Uranyl Organic Framework as a Turn-on Fluorescent pH Sensor. *Inorg. Chem.* **2020**, *59*, 1778-1784.
- [30] Feng, X.; Hu, J.-Y.; Iwanaga, F.; Seto, N.; Redshaw, C.; Elsegood, M. R. J.; Yamato, T. An Efficient Approach to the Synthesis of Novel Pyrene-Fused Azaacenes. *Org. Lett.* **2013**, *15*, 1318-1321.
- [31] Chiang, C.-L.; Tseng, S.-M.; Chen, C.-T.; Hsu, C.-P.; Shu, C.-F.; Influence of Molecular Dipoles on the Photoluminescence and Electroluminescence of Dipolar Spirobifluorenes. *Adv. Funct. Mater.* **2008**, *18*, 248–257.
- [32] Divac, V. M.; Šakić, D.; Weitner, T.; Gabričević, M.; Solvent effects on the absorption and fluorescence spectra of Zaleplon: Determination of ground and excited state dipole moments. *Spectrochim. Acta A Mol. Biomol. Spectrosc.* **2019**, *212*, 356-362.
- [33] Rajgopal, V.; Reddy, A. M.; Rao, V. J. Wavelength Dependent Trans to Cis and Quantum Chain Isomerizations of Anthrylethylene Derivatives. *J. Org. Chem.* **1995**, *60*, 7966–7973.
- [34] Gerson, F.; Huber, W.; Electron Spin Resonance Spectroscopy of Organic Radicals, WILEY-VCH Verlag GmbH & Co. KGaA, Weinheim, 2003.
- [35] Mondal, R.; Shah, B. K.; Neckers, D. C. Photogeneration of Heptacene in a Polymer Matrix. *J. Am. Chem. Soc.* **2006**, *128*, 9612-9613.
- [36] Balta, D. K.; Arsu, N.; Yagci, Y.; Sundaresan, A. K.; Jockusch, S.; Turro, N. J. Mechanism of Photoinitiated Free Radical Polymerization by Thioxanthone–Anthracene in the Presence of Air. *Macromolecules* **2011**, *44*, 2531–2535.
- [37] Falvey, D. E.; Khambatta, B. S.; Schuster, G. B. Neophyl-like rearrangement of alkoxy radicals: direct detection of a bridged intermediate by time-resolved absorption spectroscopy. *J. Phys. Chem.* **1990**, *94*, 1056–1059.
- [38] Frisch, M. J., et al. Gaussian 03, Revision C.02; Gaussian, Inc.: Wallingford, CT,

2004.

[39] Programs CrysAlis-CCD and -RED, Oxford Diffraction Ltd., Abingdon, UK (2005).

[40] Sheldrick, M.; SHELX-97 - Programs for crystal structure determination (SHELXS) and refinement (SHELXL), *Acta Cryst.* **2008**, *A64*, 112.